Hindawi Publishing Corporation
Journal of Nanomaterials
Volume 2014, Article ID 261034, 10 pages
http://dx.doi.org/10.1155/2014/261034

Research Article

Synthesis and Characterization of Structure-Controlled Micro-/Nanocomposite TiO_2 Fibers with Enhanced Photocatalytic Activity

Chengcheng Liu, Chunmei Ding, Tianyi Zhao, and Lei Jiang

School of Chemistry and Environment, Beihang University, Beijing 100191, China

Correspondence should be addressed to Tianyi Zhao; zhaoty@buaa.edu.cn

Received 23 January 2014; Accepted 9 March 2014; Published 9 April 2014

Academic Editor: Gong-Ru Lin

A series of structure-controlled composite TiO_2 fibers combining micro- and nanostructures (hereafter, micro-/nanocomposite) were fabricated using a combination of electrospinning and calcination methods, and their photocatalytic activities were investigated. Smooth microscale fibers were obtained by electrospinning a precursor solution containing tetrabutyl titanate and TiF_4. TiO_2 nanocrystals formed on the microfibers with the help of HF which was produced from the decomposition of TiF_4 in calcination. The size and quantity of TiO_2 nanocrystals can be controlled by tuning the mass ratio of TiF_4 in the sol-gel precursor solutions and the calcination time. The obtained micro-/nanocomposite TiO_2 fibers were found to exhibit enhanced photocatalytic properties when compared with the bare microfibers. These micro-/nanocomposite structures exhibit the advantages of both the nanocrystals and microfibers, which will lead to new developments in photocatalysis.

1. Introduction

Since 1972, when Fujishima and Honda found that titanium dioxide could work as photocatalyst for the decomposition of H_2O [1], many efforts have been devoted to developing heterogeneous photocatalysts for environmental applications such as air purification, water disinfection, and hazardous waste remediation [2–7]. Up to now, titanium dioxide has been proved to be one of the most suitable materials for widespread environmental applications because of its biological and chemical inertness, strong oxidizing power, cost effectiveness, and long stability against photocorrosion and chemical corrosion [8]. For example, a variety of TiO_2 materials with different morphologies such as spheres, fibers, and particles [9–16] have been fabricated to provide better photocatalytic performance in both industrial applications and chemical research. Compared with nanoparticles or nanospheres, microscale fibers can be reclaimed easily because they are more stable than nanosized structures in terms of aggregation [8]. However, microfibers are limited by their relatively smaller surface area [17] and lower photocatalytic efficiency. Therefore, fabrication of TiO_2 materials with both large surface areas and easy reclamation has become an imperative research area for many researchers.

Electrospinning has been proven to be one of the most simple and versatile methods of producing complex structures such as fibers, tubes, and films [18–23]. In this paper, composites of microscale fibers and nanoscale particles (hereafter, such structures are called micro-/nanocomposite) were prepared through two steps. First, microfibers were produced by electrospinning a precursor solution containing titanium tetrafluoride (TiF_4) and tetrabutyl titanate ($Ti(OC_4H_9)_4$). Then the as-prepared fibers were calcined at high temperature and nanocrystals formed on the surfaces of the fibers. In order to evaluate the formation mechanism of the micro-/nanocomposite fibers, a series of different mass ratios of TiF_4 in the precursor solution were used and the calcination time was changed. After further analysis of the morphology, elemental composition, and phase composition of the micro-/nanocomposite fibers obtained from the precursor solutions with different TiF_4 mass ratios, we found that the crucial factor in the fabrication was the crystallization of the TiO_2 in HF atmosphere created by the decomposition of TiF_4 during calcination. The photocatalytic activity of

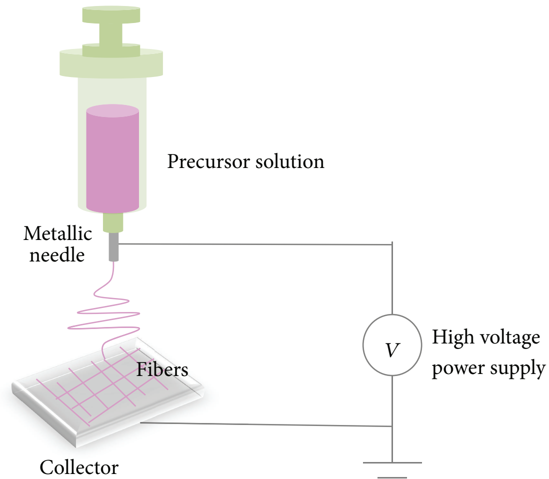

Figure 1: Illustration of electrospinning instrument.

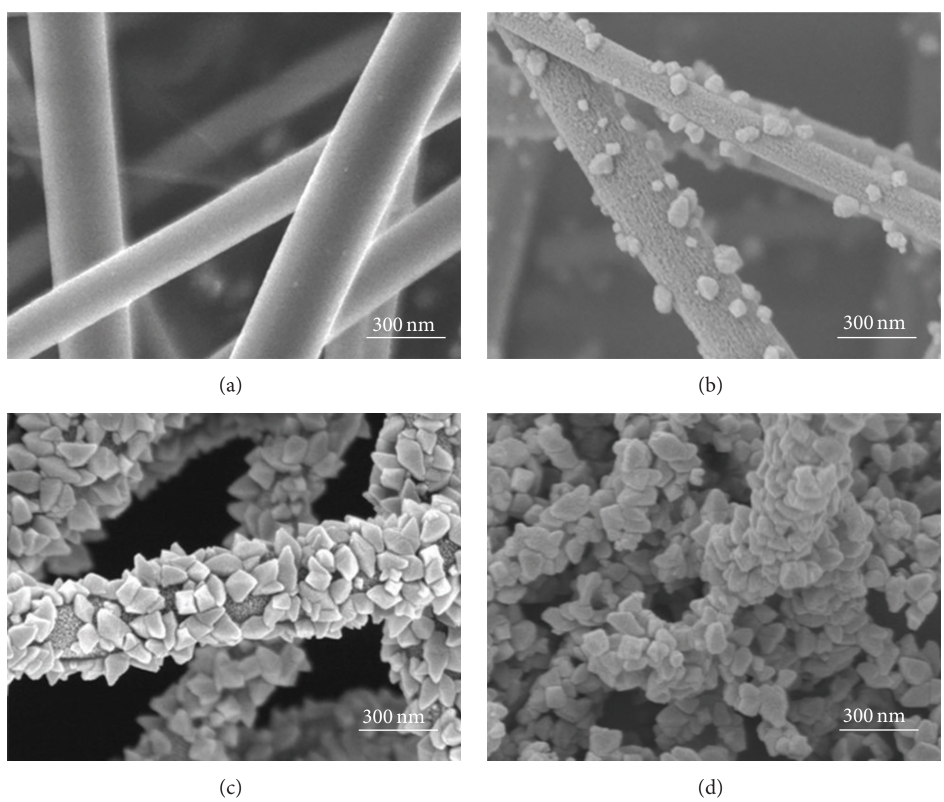

Figure 2: SEM images of micro-/nanocomposite TiO_2 fibers obtained from samples (a) F0, (b) F2, (c) F4, and (d) F6 after calcination at 500°C for 5 hours in a crucible covered with a cap.

the TiO_2 fibers was also analyzed, and it was found that such micro-/nanocomposite fibers can provide enhanced photocatalytic activity compared with smooth microscale fibers. The high surface area and the multiphase composition were responsible for the enhanced photocatalytic activity of the fibers. These micro-/nanocomposite fibers have the advantages of both the TiO_2 particles and the fibers, and they will exhibit excellent photocatalytic performance in various areas.

2. Materials and Method

2.1. Materials. Polyvinylpyrrolidone (PVP) ($M_w \approx 100000$, Aldrich Chemical Co.), tetrabutyl titanate ($Ti(OC_4H_9)_4$,

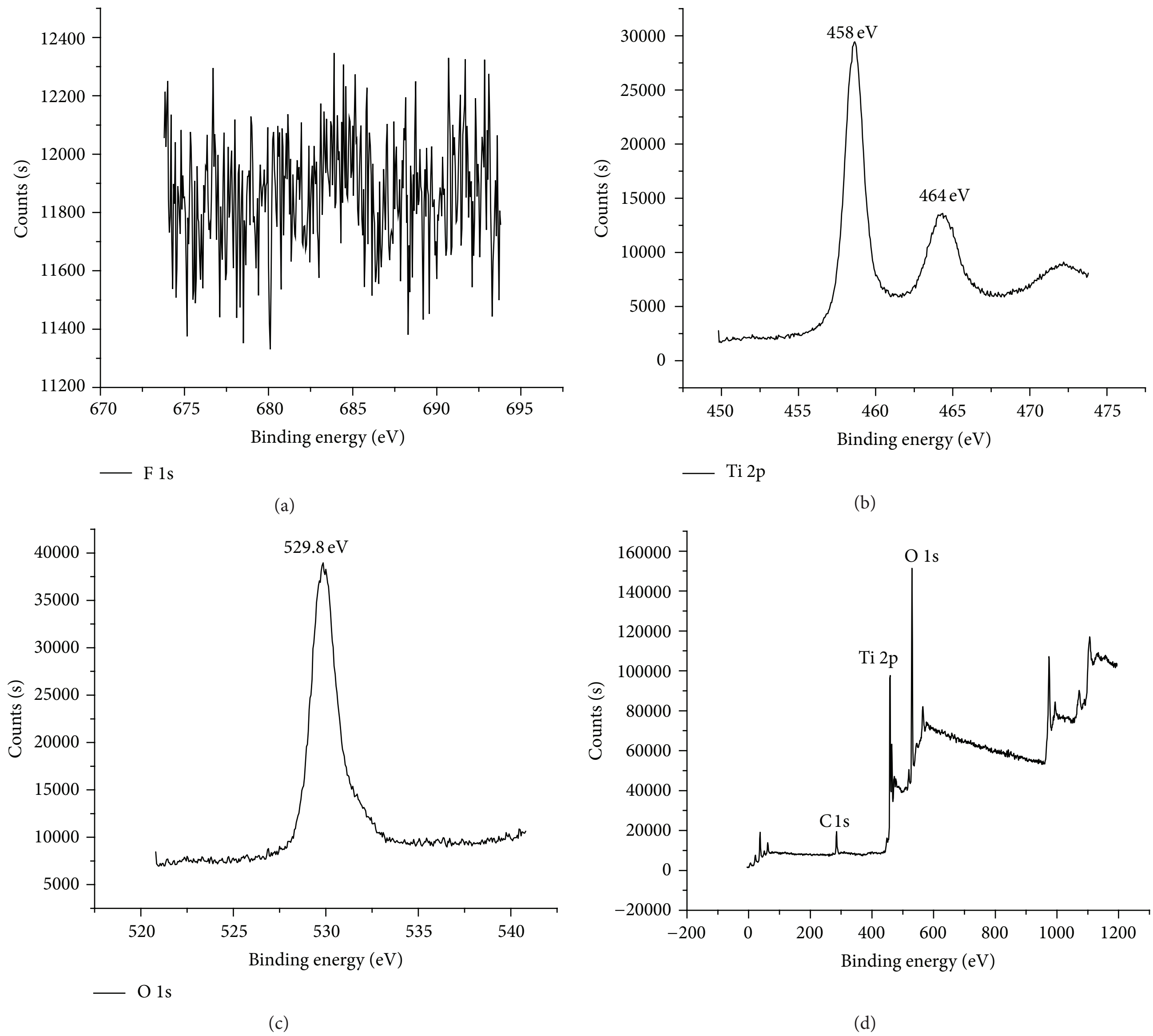

Figure 3: XPS spectra of the micro-/nanostructured TiO_2 fibers obtained from sample F4 after calcination at 500°C for 5 hours in a crucible covered with a cap: (a) F 1s, (b) Ti 2p, (c) O 1s spectra, and (d) spectrum of all elements in the fibers.

Sinopharm Chemical Reagent Co., Ltd.), titanium tetrafluoride (TiF_4, Aldrich Chemical Co.), absolute ethanol (CH_3CH_2OH, Beijing Chemical Works), acetic acid (CH_3COOH, Beijing Chemical Works), and hexadecyl trimethyl ammonium bromide ($C_{16}H_{33}(CH_3)_3NBr$ (CTAB), Fine Chemical Research Institute of Tianjin Jinke) were used as received without further purification.

2.2. Preparation of Precursor Sol-Gel Solutions. First, 12 g ethanol, 1.5 g acetic acid, 1.1 g PVP, 6 g tetrabutyl titanate, and 0.03 g CTAB were added in a capped bottle, and the solution was stirred for 0.5 hours until it became transparent. Then 0 g, 0.2 g, 0.4 g, or 0.6 g TiF_4 was added to the solution, and this mixture was continuously stirred for 0.5 hours to generate a homogeneous solution. The obtained solutions were named S0, S2, S4, and S6 according to the TiF_4 mass ratios (0 wt%, 0.96 wt%, 1.85 wt%, and 2.83 wt%) in the solution.

2.3. Microfiber Fabrication by Electrospinning. The designation of the electrospinning instrument was mainly consulted the previous work [24], which is illustrated in Figure 1. The precursor solution was loaded using an external syringe with a metallic needle, and a grounded metallic plate covered with a piece of tin foil was used as a collecting substrate. The voltage was controlled at 10–30 kV, and the work distance was 10–20 cm, depending on the conditions for each individual experiment. The obtained fibers were named F0, F2, F4, and F6 according to the TiF_4 mass ratios (0 wt%, 0.96 wt%, 1.85 wt%, and 2.83 wt%) in the precursor solution.

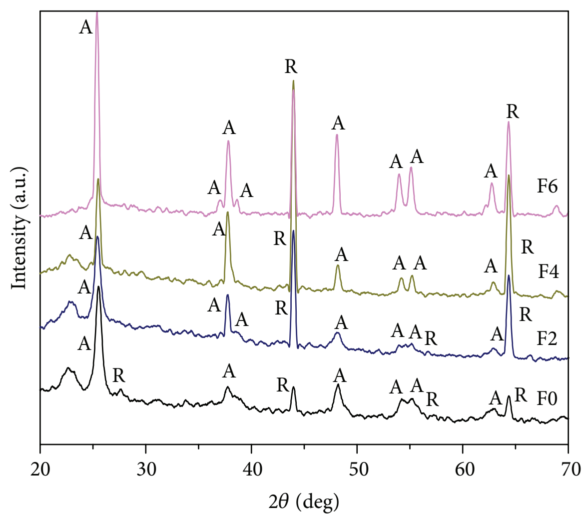

FIGURE 4: Powder X-ray diffraction patterns of micro-/nanostructured TiO_2 fibers obtained from samples F0, F2, F4, and F6 after calcination for 5 hours in a crucible covered with a cap.

2.4. Formation of Nanoparticles on Microfibers by Calcination. The electrospun products were calcined at 500°C in a crucible with a cap for 4, 5, or 6 hours. Afterwards, the micro TiO_2 fibers with nanoparticles grow on the surface were obtained. As a control experiment, the electrospun products were calcined at 500°C in air and smooth microfibers were got.

2.5. Characterization. The morphology of the TiO_2 fibers was characterized by scanning electron microscopy (SEM; JSM-6700F, JEOL, Japan). Powder X-ray diffraction (XRD) measurements were performed on a Rigaku D/Max-2500 diffractometer (Rigaku Co., Japan) with Cu Kα radiation. X-ray photoelectron spectroscopy (XPS) measurements were performed on a VG Escalab 220i XL XPS System (Thermo VG Scientific Ltd., UK). The UV-vis spectrum was obtained using a UV-vis 3100 instrument (Hitachi Co., Japan).

2.6. Photocatalytic Activity of the Micro-/Nanocomposite Fibers. The photocatalytic activity of the micro-/nanostructured fibers was evaluated by using them to catalyze the degradation of rhodamine 6G ($C_{28}H_{31}N_2O_3Cl$, Sigma Chemical Co.) in a 150 mL reactor. In each photocatalytic experiment, 0.05 g of TiO_2 fibers was used as the photocatalyst. Samples prepared from F0, F2, and F4 after calcination were selected as the photocatalysts because they could maintain their fiber morphology during the experiment and can be easily reclaimed. The initial concentration of rhodamine 6G was 1.5×10^{-5} mol/L. The changes in the concentration of rhodamine 6G during photocatalytic decomposition were monitored by in situ UV-vis spectroscopy. The system was kept in the dark for 0.5 h for adsorption equilibration and then was irradiated with UV lamps with a peak wavelength of 365 nm. The UV-vis spectrum with a 526 nm absorption peak was recorded every 30 minutes.

3. Results and Discussion

3.1. Characterization of Micro-/Nanocomposite Structured TiO_2 Fibers. Figure 2 shows the micro-/nanocomposite TiO2 fibers obtained from samples F0, F2, F4, and F6 after calcination at 500°C for 5 hours in a crucible covered with a cap. No nanoparticle formed on the surfaces of the fibers obtained from the solution without TiF_4 after calcination (Figure 2(a)), but fibers obtained from the precursor solution containing TiF_4 had nanoparticles formed on their surfaces (Figures 2(b)–2(d)). The size and quantity of the nanoparticles increase with increasing mass ratio of TiF_4 in the precursor solution. When the TiF_4 concentration in the precursor solution was sufficient (e.g., 2.83 wt%), the fibers completely transformed into nanoparticles after calcination (Figure 2(d)).

To determine the elemental composition of the micro-/nanostructured fibers, XPS spectra for the fibers obtained from sample F4 were analyzed (Figure 3). There are nearly no peaks at 684 eV and 691 eV, which means that there is no F element in the fiber (Figure 3(a)). Ti 2p region is located at 458 eV and 464 eV, indicating that the Ti element exists in the Ti^{4+} form [25]. The O 1s region is located at 530 eV, which results from the O^{2-} in the TiO_2 and hydroxyl groups on the surface of the sample [26].

As shown in Table 1, the atomic ratio of Ti and O in the fibers obtained from sample F4 is about 1 : 2, which confirms the existence of TiO_2. Therefore, we can conclude that the micro-/nanostructured fiber is mainly composed of TiO_2. In addition, as shown in Figure 3(d) and Table 1, the C 1s peak is located at 284.8 eV, which reveals that the C element exists in the micro-/nanostructured fibers. The existence of C element is probably due to the contaminant C introduced during calcination and contamination of the XPS instrument [26].

Figure 4 shows the phase composition of the different micro-/nanostructured TiO_2 fibers obtained from samples

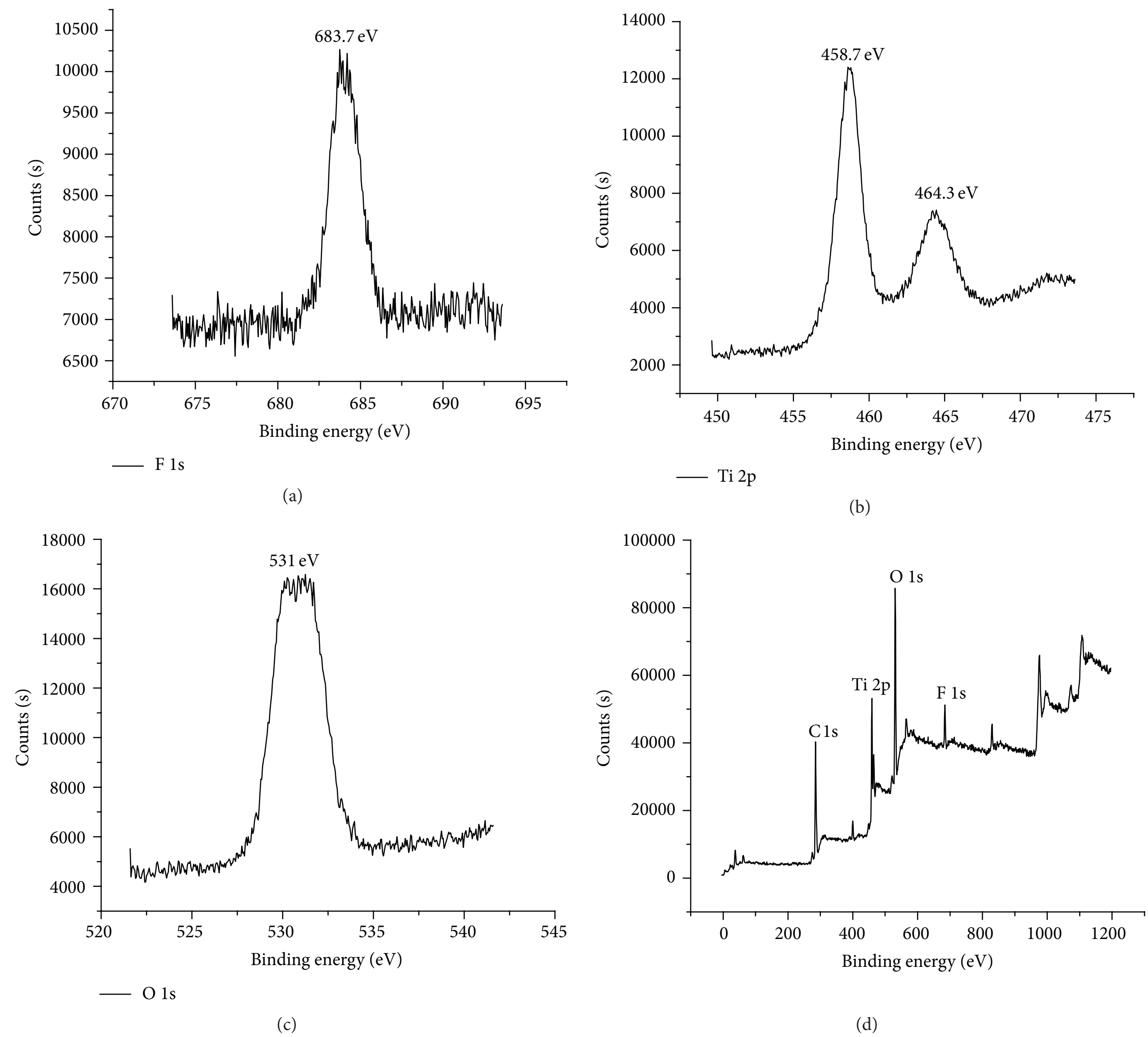

Figure 5: XPS spectra of fibers of sample F4 before calcination: (a) F 1s, (b) Ti 2p, (c) O 1s spectra, and (d) spectrum for all the elements in the fiber.

Table 1: Elements and atomic ratios of the micro-/nanostructured fibers obtained from sample F4 after calcination at 500°C for 5 hours in a crucible covered with a cap.

Elements	Atomic ratio (%)
C 1s, 284.8 eV	18.91
O 1s, 529.7 eV	57.39
Ti 2p, 458.4 eV	23.7

F0, F2, F4, and F6. From Figure 4, we can see that different samples of TiO_2 fibers exhibited similar mixed anatase and rutile phases (PDF cards 75–1537 and 75–1755, JCPDS). The peaks attributed to the TiO_2 anatase and rutile phases become stronger with increasing TiF_4 mass ratio in the precursor solution.

3.2. Mechanism of the Formation of Micro-/Nanocomposite TiO_2 Fibers. Before calcination but after electrospinning, XPS results of the obtained fibers show that there is an F 1s peak located at 683.7 eV (Figure 5(a)), which could be attributed to F^- ions physically adsorbed on the surfaces of the fibers [27, 28]. The Ti 2p peaks are located at 458.7 eV and 464.3 eV, which shows that the Ti element is in the Ti^{4+} form. The O 1s region is located at 531 eV, which results from the O^{2-} in the TiO_2 and hydroxyl groups on the surface of the sample. Therefore, before calcination, TiF_4, HF, and TiO_2 are probably present in the fibers. After calcination in air, we only obtained

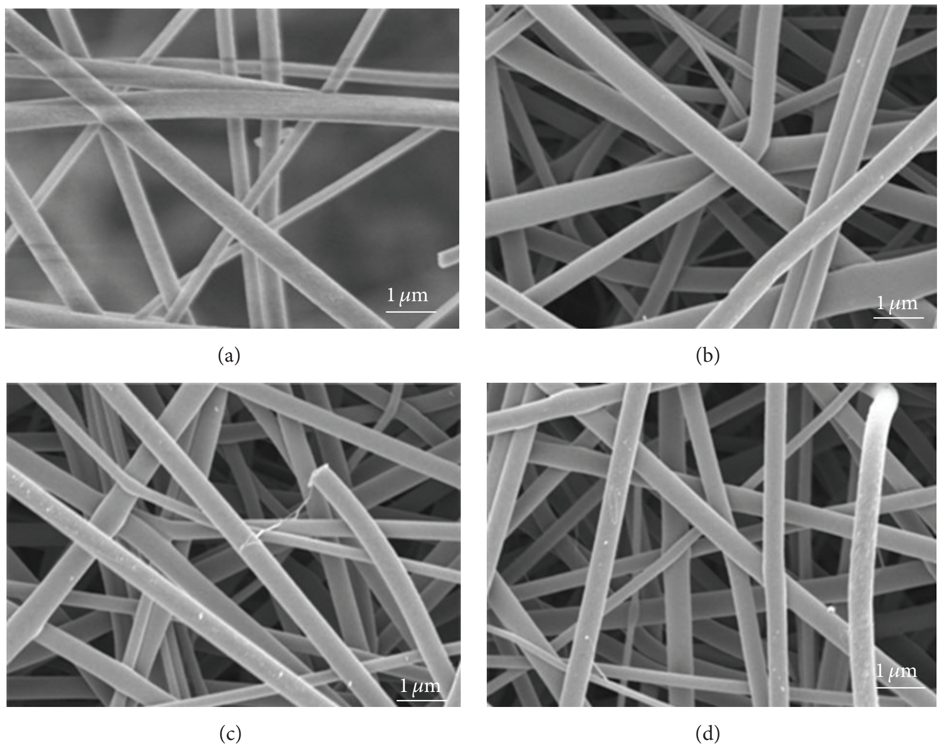

Figure 6: SEM images of fibers obtained from samples (a) F0, (b) F2, (c) F4, and (d) F6 after calcination at 500°C for 5 hours in air.

smooth fibers (Figure 6). The XPS results showed that there was no F in the smooth fibers, because there is no peak at 684 eV or 691 eV (Figure 7(a)). The smooth fibers were mainly composed of TiO_2 because Ti element is mainly in the Ti^{4+} form and O is mainly in the O^{2-} form (Figures 7(b)–7(d)). When calcination was carried out in a crucible covered with a cap, micro-/nanostructured TiO_2 fibers formed, in which there was also no F element.

From all of these facts, we deduce that, during the electrospinning and calcination, the TiF_4 in the fibers obtained from the precursor solution hydrolyzes by moisture in the air and HF is produced:

$$TiF_4 + 2H_2O \longrightarrow TiO_2 + 4HF \quad (1)$$

In air, the density of HF is low and it has little influence on the fibers. However, when the fiber is calcined in a crucible covered with a cap, the density of HF can be kept relatively high. Absorption of HF is known to be beneficial for the formation of TiO_2 crystals [29–31], so micro-/nanostructured TiO_2 fibers are obtained after calcination in a crucible covered with a cap. The more TiF_4 there is in the precursor solution, the higher the HF density is in the calcination process. Therefore fibers obtained from precursor solutions containing more TiF_4 will have more nanocrystals formed on the surface. In our experiment, sample F6 has a high TiF_4 mass ratio and, in the calcination process, the majority of TiO_2 once in the fiber morphology will gradually be transformed into nanocrystals with the assistance of the high HF density atmosphere. Therefore the samples obtained from fibers F6 are mainly composed of nanocrystals and cannot maintain the nanoparticle-on-fiber morphology any more (Figure 2(d)).

We further investigated the effect of calcination time on the formation of micro-/nanostructured fibers. Figure 8 shows SEM images of the micro-/nanostructured fibers obtained from samples F4 after calcination for 4, 5, and 6 hours. All of these samples exhibited the micro-/nanostructure, and the quantity of nanoparticles increased with increasing calcination time. When the calcination time was 6 hours, the TiO_2 once constructed for the fibers has grown into nanoparticles; therefore the surfaces of the samples were entirely composed of nanoparticles.

The powder X-ray diffraction (XRD) patterns (Figure 9) show that the anatase and rutile phase peaks of the micro-/nanostructured fibers increase in intensity with the increasing of calcination time, which means that a longer calcination time is beneficial for the crystallization of TiO_2 fibers. The reason for this can be explained as follows: as for fibers calcined for a long time, the HF produced from the decomposition of TiF_4 will have a long time to react with the TiO_2 fibers, so there will be more TiO_2 crystals formed on the fiber surfaces.

3.3. Enhanced Photocatalytic Ability of the Micro-/Nanostructured TiO_2 Fibers. Figure 10 shows the UV-vis absorption spectra of the micro-/nanocomposite TiO_2 fibers obtained from precursor solutions with different mass ratios of TiF_4. Compared with the smooth TiO_2 fibers (fibers obtained from sample F0 after calcination), there is no obvious shift in the fundamental absorption edge of the

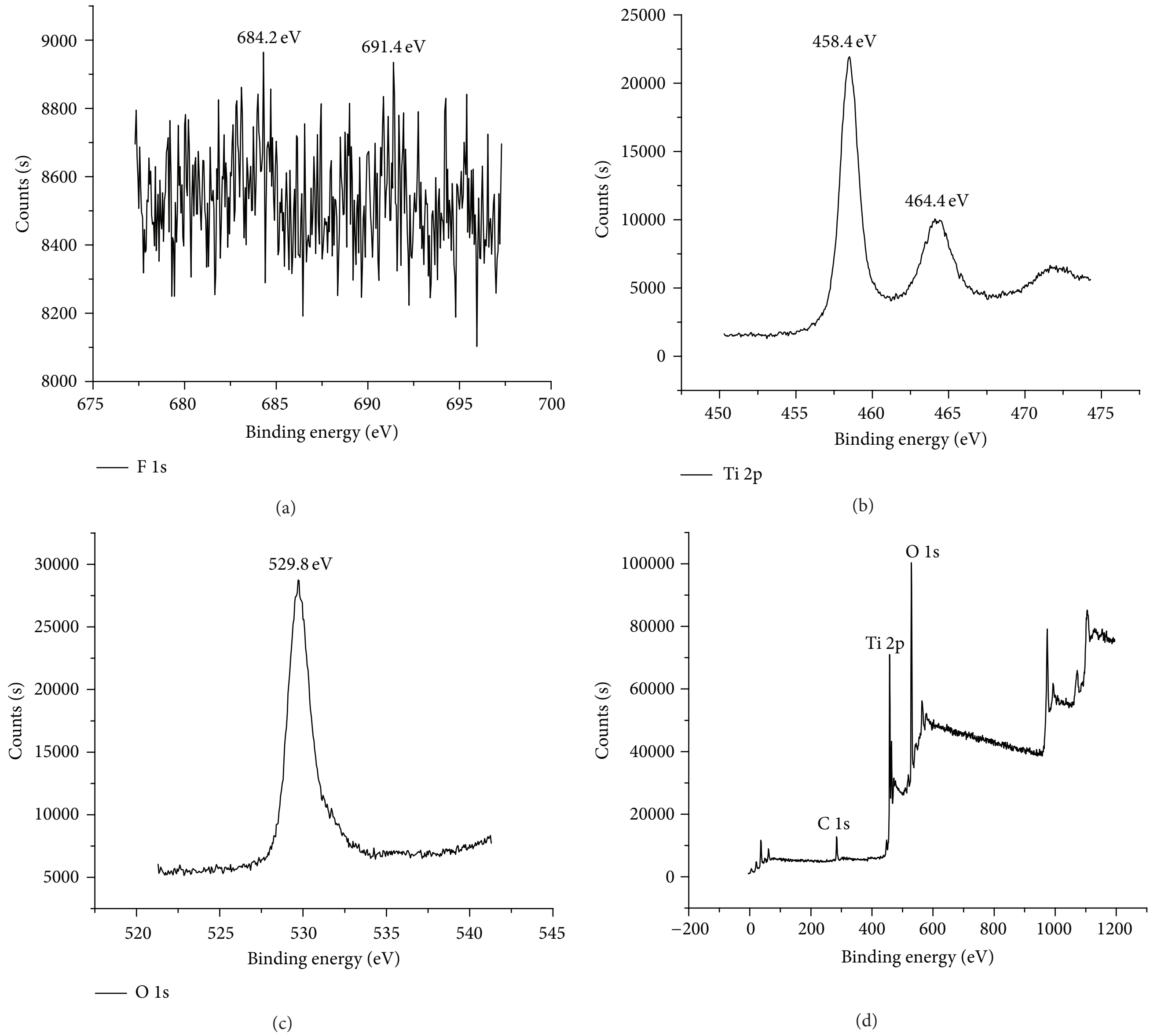

Figure 7: XPS spectra of sample F4 after calcination at 500°C for 5 hours in air: (a) F 1s, (b) Ti 2p, (c) O 1s spectra, and (d) spectrum for all the elements in the fiber.

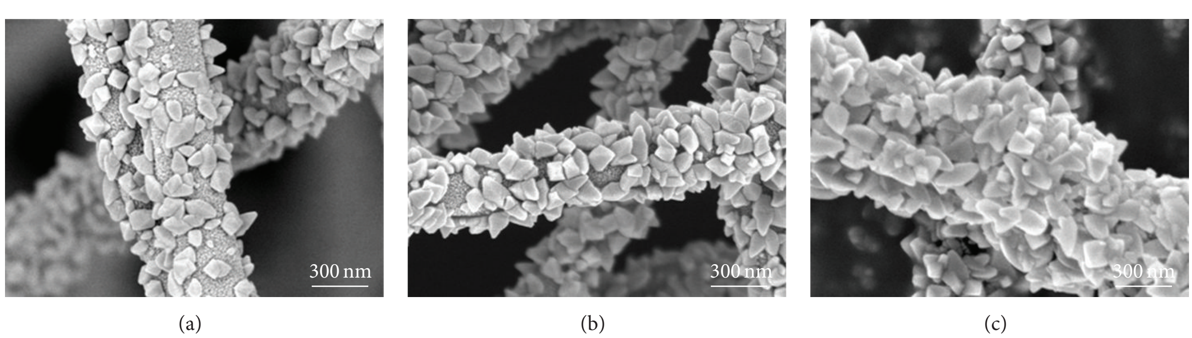

Figure 8: SEM images of micro-/nanostructured fibers obtained from sample F4 after calcination in a crucible covered with a cap at 500°C for different times: (a) 4 hours, (b) 5 hours, and (c) 6 hours.

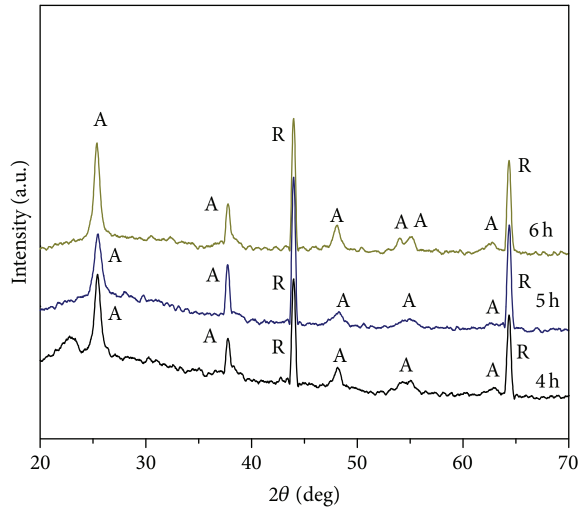

Figure 9: Powder X-ray diffraction patterns of micro-/nanostructured fibers obtained from sample F4 after calcination in a crucible covered with a cap at 500°C for 4, 5, and 6 hours.

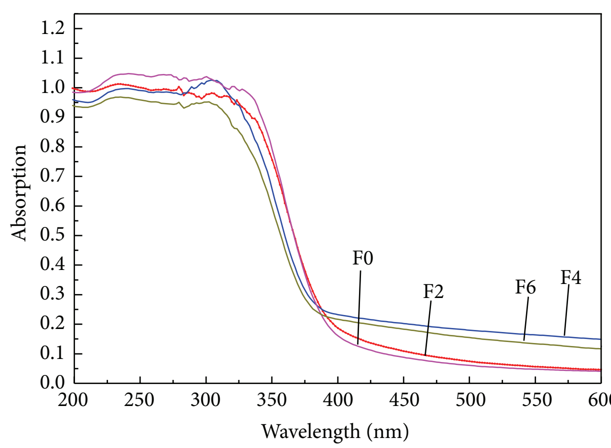

Figure 10: UV-vis absorption spectrum of the micro-/nanostructured fibers obtained from samples F0, F2, F4, and F6 after calcination for 5 hours in a sealed crucible.

micro-/nanostructured TiO_2 fibers (fibers obtained from F2, F4, and F6 after calcination). The micro-/nanostructured TiO_2 fibers obtained from samples of F2, F4, and F6 showed enhanced light absorption at wavelengths larger than 350 nm, which is probably due to the C elements in the micro-/nanostructured fibers (Figure 3(d)).

The photocatalytic activity of the micro-/nanostructured TiO_2 fibers was evaluated by using them to catalyze the degradation of rhodamine 6G. For each fiber sample, we calculated the initial rate constant (k) of rhodamine 6G degradation. The photocatalytic degradation of rhodamine 6G by TiO_2 is found to follow first-order kinetics, because the plot of $\ln(C_0/C_t)$ versus photocatalytic reaction time in our experiment is linear (Figure 11). Here C_t is the concentration of rhodamine 6G after a photocatalytic reaction time t in minutes, and C_0 is the initial concentration of rhodamine 6G. According to Figure 11, we obtained k(F0), k(F2), and k(F4) as −0.003, −0.00493, and −0.008, respectively. The absolute value of k(F4) is larger than that of k(F2), and the absolute value of k(F2) is larger than that of k(F0), so we can conclude that the initial rate constant for rhodamine 6G degradation increases with increasing number of nanocrystals on the fibers. This means that the photocatalytic activity of the micro-/nanostructured fibers increases with the quantity of nanocrystals on the fibers.

3.4. Mechanism for the Enhanced Photocatalysis of the Micro-/Nanostructured Fibers. We analyzed the difference between the smooth TiO_2 microfibers and the micro-/nanostructured TiO_2 fibers and arrived at the following reasons for the enhanced photocatalytic ability of the micro-/nanostructured fibers. First, the TiO_2 nanocrystals on the surface of the fiber lead to a high surface area, which is beneficial to the photocatalytic activities because it provides a large reactive area and facilitates the absorption of the target species, which is rhodamine 6G in our case [32]. Therefore, the larger

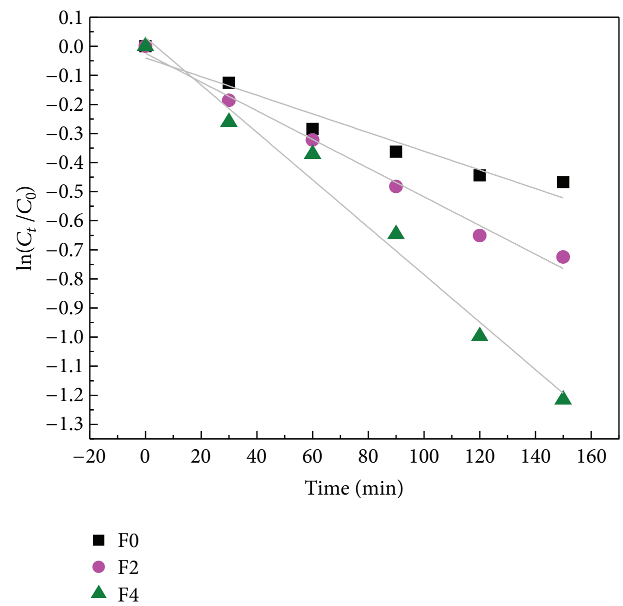

FIGURE 11: Kinetics data for the degradation of rhodamine 6G over micro-/nanostructured TiO_2 fibers obtained from samples F0, F2, and F4.

the surface area is, the higher catalytic efficiency the photocatalyst shows. Second, the micro-/nanocomposite fibers are composed of TiO_2 in anatase and rutile phases. The different band edges of these two phases help facilitate the charge separation and election transfer in the photocatalytic process [33] and the multiphase composition in our sample could enhance the catalytic efficiency of the photocatalysts [34]. Therefore, the augment of the photocatalytic activity of the micro-/nanostructured fibers can be attributed to both the enlargement of surface area and the multiphase composition of TiO_2.

4. Conclusions

In summary, we successfully fabricated micro-/nanocomposite TiO_2 fibers using the electrospinning method and calcination. The nanoparticles resulted from the decomposition of the TiF_4 in the fibers left over from the precursor solutions. By changing the TiF_4 mass ratio in the precursor solution and the calcination time, we can control the quantity and size of the nanoparticles. The micro-/nanostructured TiO_2 fibers exhibited enhanced photocatalytic activity compared with smooth TiO_2 fibers because of the high surface area provided by the nanoparticles and the complex anatase and rutile phase composition. Since the micro-/nanostructured TiO_2 fibers exhibit enhanced photocatalytic activity and can be reclaimed easily, they will exhibit excellent photocatalytic performance for various applications.

Conflict of Interests

The authors declare that there is no conflict of interests regarding the publication of this paper.

Acknowledgments

The authors thank the National Natural Science Foundation of China (Grant no. 21101010) and the Innovation Foundation of BUAA for Ph.D. Graduates (296181) for continuing financial support.

References

[1] A. Fujishima and K. Honda, “Electrochemical photolysis of water at a semiconductor electrode,” *Nature*, vol. 238, no. 5358, pp. 37–38, 1972.

[2] K. Vinodgopal, D. E. Wynkoop, and P. V. Kamat, “Environmental photochemistry on semiconductor surfaces: photosensitized degradation of a textile azo dye, Acid Orange 7, on TiO_2 particles using visible light,” *Environmental Science and Technology*, vol. 30, no. 5, pp. 1660–1666, 1996.

[3] I. M. Butterfield, P. A. Christensen, A. Hamnett et al., “Applied studies on immobilized titanium dioxide films as catalysts for the photoelectrochemical detoxification of water,” *Journal of Applied Electrochemistry*, vol. 27, no. 4, pp. 385–395, 1997.

[4] D. Y. Goswami, D. M. Trivedi, and S. S. Block, “Photocatalytic disinfection of indoor air,” *Journal of Solar Energy Engineering, Transactions of the ASME*, vol. 119, no. 1, pp. 92–96, 1997.

[5] I. Sopyan, M. Watanabe, S. Murasawa, K. Hashimoto, and A. Fujishima, “An efficient TiO_2 thin-film photocatalyst: photocatalytic properties in gas-phase acetaldehyde degradation,” *Journal of Photochemistry and Photobiology A: Chemistry*, vol. 98, no. 1-2, pp. 79–86, 1996.

[6] S. Sato and J. M. White, “Photodecomposition of water over Pt/TiO_2 catalysts,” *Chemical Physics Letters*, vol. 72, no. 1, pp. 83–86, 1980.

[7] A. Hässelbarth, A. Eychmüller, R. Eichberger, M. Giersig, A. Mews, and H. Weller, “Chemistry and photophysics of mixed

CdS/HgS colloids," *Journal of Physical Chemistry*, vol. 97, no. 20, pp. 5333–5340, 1993.

[8] G. Wu, J. Wang, D. F. Thomas, and A. Chen, "Synthesis of F-doped flower-like TiO_2 nanostructures with high photoelectrochemical activity," *Langmuir*, vol. 24, no. 7, pp. 3503–3509, 2008.

[9] Y. Zhao, X. Cao, and L. Jiang, "Bio-mimic multichannel microtubes by a facile method," *Journal of the American Chemical Society*, vol. 129, no. 4, pp. 764–765, 2007.

[10] J. M. Macák, H. Tsuchiya, and P. Schmuki, "High-aspect-ratio TiO_2 nanotubes by anodization of titanium," *Angewandte Chemie*, vol. 44, no. 14, pp. 2100–2102, 2005.

[11] D. Li and Y. Xia, "Fabrication of titania nanofibers by electrospinning," *Nano Letters*, vol. 3, no. 4, pp. 555–560, 2003.

[12] D. Li and Y. Xia, "Direct fabrication of composite and ceramic hollow nanofibers by electrospinning," *Nano Letters*, vol. 4, no. 5, pp. 933–938, 2004.

[13] X. Huang and Z. Liu, "Heterogeneous deposition of Cu_2 O nanoparticles on TiO_2 nanotube array films in organic solvent," *Journal of Nanomaterials*, vol. 2013, Article ID 517648, 8 pages, 2013.

[14] J. Qu and C. Lai, "One-dimensional TiO_2 nanostructures as photoanodes for dye-sensitized solar cells," *Journal of Nanomaterials*, vol. 2013, Article ID 762730, 11 pages, 2013.

[15] S. Wang, T. Wang, Y. W. Ding et al., "Gas-supported high-photoactivity TiO_2 nanotubes," *Journal of Nanomaterials*, vol. 2012, Article ID 909473, 6 pages, 2012.

[16] T. Y. Zhao, Y. Zhao, and L. Jiang, "Nano-/microstructure improved photocatalytic activities of semiconductors," *Philosophical Transactions of the Royal Society A: Physical, Mathematical and Engineering Sciences*, vol. 371, no. 2000, Article ID 20120303, 2013.

[17] T. Y. Zhao, Z. Y. Liu, K. Nakata et al., "Multichannel TiO_2 hollow fibers with enhanced photocatalytic activity," *Journal of Materials Chemistry*, vol. 20, no. 24, pp. 5095–5099, 2010.

[18] A. C. Patel, S. Li, J.-M. Yuan, and Y. Wei, "In situ encapsulation of horseradish peroxidase in electrospun porous silica fibers for potential biosensor applications," *Nano Letters*, vol. 6, no. 5, pp. 1042–1046, 2006.

[19] J. A. Matthews, G. E. Wnek, D. G. Simpson, and G. L. Bowlin, "Electrospinning of collagen nanofibers," *Biomacromolecules*, vol. 3, no. 2, pp. 232–238, 2002.

[20] R. A. Caruso, J. H. Schattka, and A. Greiner, "Titanium dioxide tubes from Sol-Gel coating of electrospun polymer fibers," *Advanced Materials*, vol. 13, no. 20, pp. 1577–1579, 2001.

[21] L. Jiang, Y. Zhao, and J. Zhai, "A lotus-leaf-like superhydrophobic surface: a porous microsphere/nanofiber composite film prepared by electrohydrodynamics," *Angewandte Chemie*, vol. 43, no. 33, pp. 4338–4341, 2004.

[22] Y. Zhu, J. Zhang, Y. Zheng, Z. Huang, L. Feng, and L. Jiang, "Stable, superhydrophobic, and conductive polyaniline/polystyrene films for corrosive environments," *Advanced Functional Materials*, vol. 16, no. 4, pp. 568–574, 2006.

[23] Y. Zhao, J. Zhai, S. Tan, L. Wang, L. Jiang, and D. Zhu, "TiO_2 micro/nano-composite structured electrodes for quasi-solid-state dye-sensitized solar cells," *Nanotechnology*, vol. 17, no. 9, pp. 2090–2097, 2006.

[24] M. W. Lee, S. An, S. S. Latthe, C. Lee, S. Hong, and S. S. Yoon, "Electrospun polystyrene nanofiber membrane with superhydrophobicity and superoleophilicity for selective separation of water and low viscous oil," *ACS Applied Materials & Interfaces*, vol. 5, no. 21, pp. 10597–10604, 2013.

[25] B. M. Reddy, K. N. Rao, G. K. Reddy, and P. Bharali, "Characterization and catalytic activity of V_2O_5/Al_2O_3-TiO_2 for selective oxidation of 4-methylanisole," *Journal of Molecular Catalysis A: Chemical*, vol. 253, no. 1-2, pp. 44–51, 2006.

[26] C. Yu, D. Cai, K. Yang, J. C. Yu, Y. Zhou, and C. Fan, "Sol-gel derived S,I-codoped mesoporous TiO_2 photocatalyst with high visible-light photocatalytic activity," *Journal of Physics and Chemistry of Solids*, vol. 71, no. 9, pp. 1337–1343, 2010.

[27] D. Li, H. Haneda, N. K. Labhsetwar, S. Hishita, and N. Ohashi, "Visible-light-driven photocatalysis on fluorine-doped TiO_2 powders by the creation of surface oxygen vacancies," *Chemical Physics Letters*, vol. 401, no. 4-6, pp. 579–584, 2005.

[28] J. C. Yu, J. Yu, W. Ho, Z. Jiang, and L. Zhang, "Effects of F-doping on the photocatalytic activity and microstructures of nanocrystalline TiO_2 powders," *Chemistry of Materials*, vol. 14, no. 9, pp. 3808–3816, 2002.

[29] A. S. Barnard and L. A. Curtiss, "Prediction of TiO_2 nanoparticle phase and shape transitions controlled by surface chemistry," *Nano Letters*, vol. 5, no. 7, pp. 1261–1266, 2005.

[30] Y. W. Jun, M. F. Casula, J. H. Sim, S. Y. Kim, J. Cheon, and A. P. Alivisatos, "Surfactant-assisted elimination of a high energy facet as a means of controlling the shapes of TiO_2 nanocrystals," *Journal of the American Chemical Society*, vol. 125, no. 51, pp. 15981–15985, 2003.

[31] H. G. Yang, C. H. Sun, S. Z. Qiao et al., "Anatase TiO_2 single crystals with a large percentage of reactive facets," *Nature*, vol. 453, no. 7195, pp. 638–641, 2008.

[32] J. Li, J. Xu, W.-L. Dai, H. Li, and K. Fan, "Direct hydro-alcohol thermal synthesis of special core-shell structured Fe-doped titania microspheres with extended visible light response and enhanced photoactivity," *Applied Catalysis B: Environmental*, vol. 85, no. 3-4, pp. 162–170, 2009.

[33] D. Yang, H. Liu, Z. Zheng et al., "An efficient photocatalyst structure: TiO_2(B) nanofibers with a shell of anatase nanocrystals," *Journal of the American Chemical Society*, vol. 131, no. 49, pp. 17885–17893, 2009.

[34] D. Zhang, G. Li, X. Yang, and J. C. Yu, "A micrometer-size TiO_2 single-crystal photocatalyst with remarkable 80% level of reactive facets," *Chemical Communications*, no. 29, pp. 4381–4383, 2009.

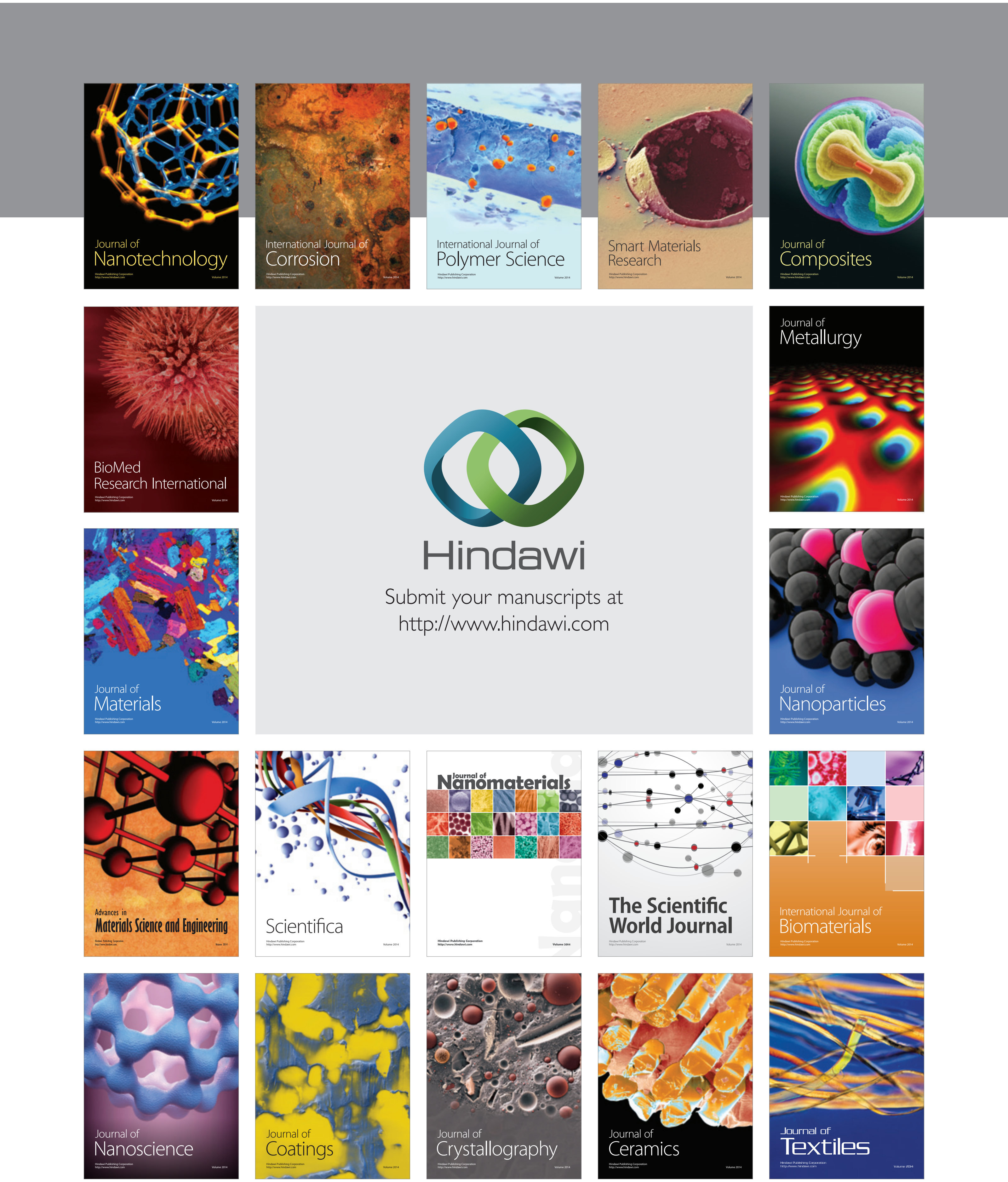
Journal of
Nanotechnology
International Journal of
Corrosion
International Journal of
Polymer Science
Smart Materials
Research
Journal of
Composites
BioMed
Research International
Hindawi
Submit your manuscripts at
http://www.hindawi.com
Journal of
Metallurgy
Journal of
Materials
Journal of
Nanoparticles
Advances in
Materials Science and Engineering
Scientifica
Journal of
Nanomaterials
The Scientific
World Journal
International Journal of
Biomaterials
Journal of
Nanoscience
Journal of
Coatings
Journal of
Crystallography
Journal of
Ceramics
Journal of
Textiles